INSTITUTE OF PHYSICS PUBLISHING JOURNAL OF PHYSICS: CONDENSED MATTER
J. Phys.: Condens. Matter **16** (2004) 785–798 PII: S0953-8984(04)69662-7

Melting of sodium clusters in electron irradiated NaCl

A V Sugonyako[1], D I Vainshtein[1], A A Turkin[2], H W den Hartog[1,4] and A A Bukharaev[3]

[1] Solid State Physics Laboratory, University of Groningen, Nijenborgh 4, NL-9747 AG Groningen, The Netherlands
[2] National Science Centre, 'Kharkov Institute of Physics and Technology', 61108 Kharkov, Ukraine
[3] Zavoisky Physical Technical Institute of Russian Academy of Sciences, Kazan, 420029, Russia

E-mail: sugonyako@phys.rug.nl, d.vainshtein@phys.rug.nl, anatole.turkin@kipt.kharkov.ua, a.turkin@phys.rug.nl, h.w.den.hartog@phys.rug.nl and bukh@kfti.knc.ru

Received 26 September 2003
Published 30 January 2004
Online at stacks.iop.org/JPhysCM/16/785 (DOI: 10.1088/0953-8984/16/6/009)

Abstract

In this paper we present the results of the first systematic investigation of the geometrical properties of sodium nanoclusters in NaCl using the combined results of differential scanning calorimetry (DSC) and atomic force microscopy (AFM). The melting behaviour of the sodium nanoclusters which had been produced in NaCl by electron beam irradiation up to a dose of 200 MGy has been studied by means of DSC. The sodium colloids have been visualized by AFM and their size distribution has been evaluated for two irradiation doses. The DSC scans of the irradiated samples exhibit two melting peaks located at temperatures below the melting temperature of bulk sodium. A phenomenological model has been proposed which explains this behaviour by the existence of two different structural states in the population of sodium colloids. We believe that small sodium clusters inherit the FCC structure from the surrounding Na sublattice in the NaCl matrix. When a small colloid grows, its lattice structure eventually transforms into the BCC structure of bulk sodium. The model results have been compared with the DSC measurements and the transition radius for the two structural states has been estimated.

1. Introduction

The study of the thermal properties and melting behaviour of small metallic clusters has become a highly active field of research in the past few years. Many recent experimental results and theoretical calculations show the intricate dependence of the melting point on the size of free metallic clusters [1–4]. In this paper we present experimental observations of sodium clusters,

[4] Author to whom any correspondence should be addressed.

which have been produced in bulk NaCl by the exposure of the samples to an intense beam of high-energy electrons from an electron accelerator. We also present the results of the first systematic investigation of the geometrical properties of sodium nanoclusters in NaCl using the combined results of differential scanning calorimetry (DSC) and atomic force microscopy (AFM). To achieve this we have combined calorimetrical and microscopical studies of metallic clusters in exactly the same samples. Sodium clusters were visualized on the cleaved surface of irradiated NaCl crystals by AFM. DSC has been used for the investigation of the thermal properties of radiation-induced sodium clusters. It should be taken into account that the melting properties of free clusters and clusters embedded in an ionic crystalline lattice are different. In the latter case the clusters are affected by the presence of the surrounding matrix. Another complication in our investigation is that we are dealing with clusters with varying sizes distributed in some interval.

Several sets of K doped NaCl mono-crystalline samples have been irradiated by means of 1.35 MeV electrons from a van de Graaff accelerator to doses between 50 and 200 MGy (2×10^{17} and 8×10^{17} e^{-} cm^{-2}). Details of the experimental setup have been described in [12]. The irradiation dose in the sample is homogeneous [12]. The irradiation dose in the irradiated sample has been calculated using standard procedures [13]. The samples have been selected for investigation on the basis of our previous results [5]. In various stages of the irradiation isolated sodium clusters (or colloids) show the features of nucleation and growth with increasing irradiation up to the ultimate dose values mentioned above.

2. Experiment

2.1. Differential scanning calorimetry

DSC measurements have been carried out to investigate the samples. This method is very suitable for the determination of the volume fraction of metallic Na produced inside the sample during the irradiation process. The latent heat of melting (LHM) of the Na colloids has been measured for each sample with a Perkin-Elmer DSC-7 system. The difference in heat flow between the irradiated sample and the reference sample (unirradiated NaCl) was measured during heating from 50 to 150 °C with a heating rate of 10 °C min^{-1}. The appearance of the LHM peaks in the 'DSC spectrum' (i.e. the difference between the irradiated and unirradiated NaCl samples) in this temperature interval is evidence for the presence of sodium colloids in the sample.

For the samples used in this investigation we have observed two melting peaks in the 'DSC spectrum', namely, at 82 °C (peak 1) and 92 °C (peak 2) (figure 1). These positions are the mean values for all studied samples which exhibit a scatter of ±2 °C. This is in good agreement with our previous results [5]. A detailed analysis of the DSC spectra for samples with different irradiation doses has also been presented in [5].

The LHM of Na has been calculated for each sample from the DSC curves. Based on the LHM values for Na we have calculated the total amount of metallic Na in each sample. For all samples these parameters are presented in table 1.

2.2. Atomic force microscopy

The AFM results were obtained in ultra high vacuum (UHV) using an UHV AFM/STM Omicron system in the non-contact mode. To avoid chemical reactions between the radiolytic Na colloids and oxygen or water, the irradiated samples were cleaved, prepared and kept under UHV conditions prior to and during the experiments. Several AFM images have been obtained

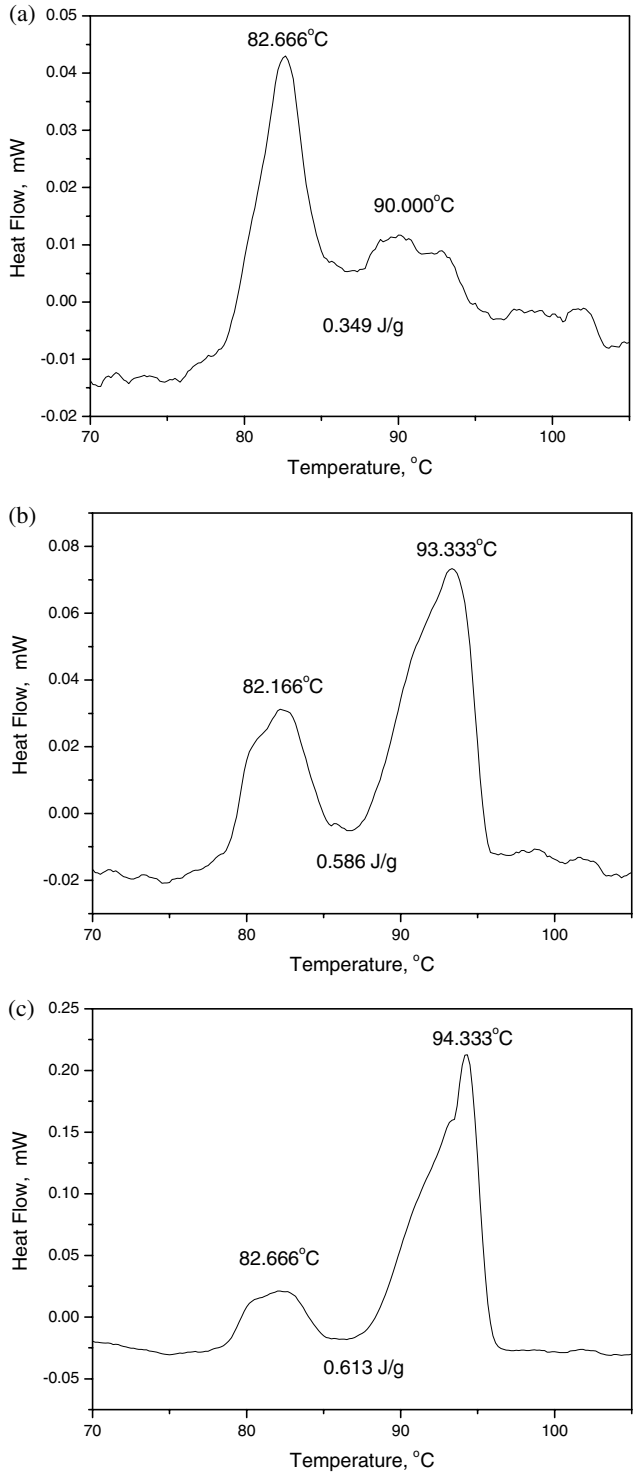

Figure 1. DSC spectra of NaCl samples irradiated up to different doses at irradiation temperatures 100 and 120 °C. (a) 50 MGy, $T_{irr} = 120\,^{\circ}C$, (b) 150 MGy, $T_{irr} = 100\,^{\circ}C$, (c) 200 MGy, $T_{irr} = 100\,^{\circ}C$.

Table 1. Parameters of the investigated samples. The irradiation doses, the irradiation temperatures, and the thermal characteristics of the samples (i.e. the LHM and the associated Na volume fraction).

Sample	Matrix and dopant	Dose (MGy) ($e^- cm^{-2}$)	Irradiation temperature (°C)	Latent heat of melting (J g^{-1})	Volume fraction of metallic Na (%)
I	NaCl + 1000 ppm potassium chloride	50 (2×10^{17})	120	0.349	0.691
II		100 (4×10^{17})	100	0.347	0.687
III		150 (6×10^{17})	100	0.586	1.160
IV		200 (8×10^{17})	100	0.613	1.214
V		200 (8×10^{17})	130	0.718	1.422

from different areas for each sample. As expected, we have observed sodium colloids with different sizes for all samples. AFM images for each of the samples are presented in figure 2. The radii of AFM tips, used in this investigation, have been estimated to be in the range between 20 and 30 nm.

The distributions of the particle sizes have been obtained from an analysis of the AFM images. An image analysis allows us to measure two size characteristics of the nanoparticles: (i) the height of protrusions in the profile measured perpendicular to the cleaved surface (along the z-direction—Z-size), and (ii) the lateral radii of protrusions along the x- and y-directions. We have found that the protrusion height changes from 0.5 to 30 nm, while the lateral diameter at half-height varies between 5 and 100 nm.

Here we expect to have strong convolution effects: first, because the radius of the measuring tip (20–30 nm) is much larger than the average lateral size of the nanoparticles. This implies that in the image the lateral sizes are significantly larger than the real ones. Second, the different interactions between the AFM tip and the different materials (metallic Na and insulating NaCl) at the surface of the cleaved sample might disturb the AFM image. The calculation of these effects is quite an intricate problem, which is beyond the scope of this paper. Therefore, we have used the Z-size of the nanoparticle-particles as a more reliable parameter for the evaluation of the colloid radii.

The size distributions of the Na nanoparticles obtained from our analysis are presented in the histograms shown in figure 3. For all samples the height and width distributions were found by accumulating the results for five different 1000 nm $\times$ 1000 nm images obtained from the same sample.

The distributions of the protrusion heights as well as the lateral sizes can be represented by the corresponding histograms. The distribution functions show a clear dependence on irradiation dose. Starting with a rather narrow peak centred at about 3 nm (observed for the relatively low dose 50 MGy sample) the width of the asymmetric distribution of Z-sizes increases with increasing irradiation dose. In addition, with increasing irradiation dose the average value of the asymmetric size distribution shifts slowly to larger sizes.

As expected the lateral sizes are several times larger than real ones, but at least qualitatively the same tendency as observed for the Z-sizes can be recognized here.

3. Reconstruction of the size distribution function of the sodium colloids using the AFM data

The AFM data obtained in this investigation has been used to reconstruct the volume size distribution of sodium colloids. Mathematically, the problem is formulated as follows. Let the 3D medium (NaCl matrix) contain spherical objects (colloid particles) with a size distribution

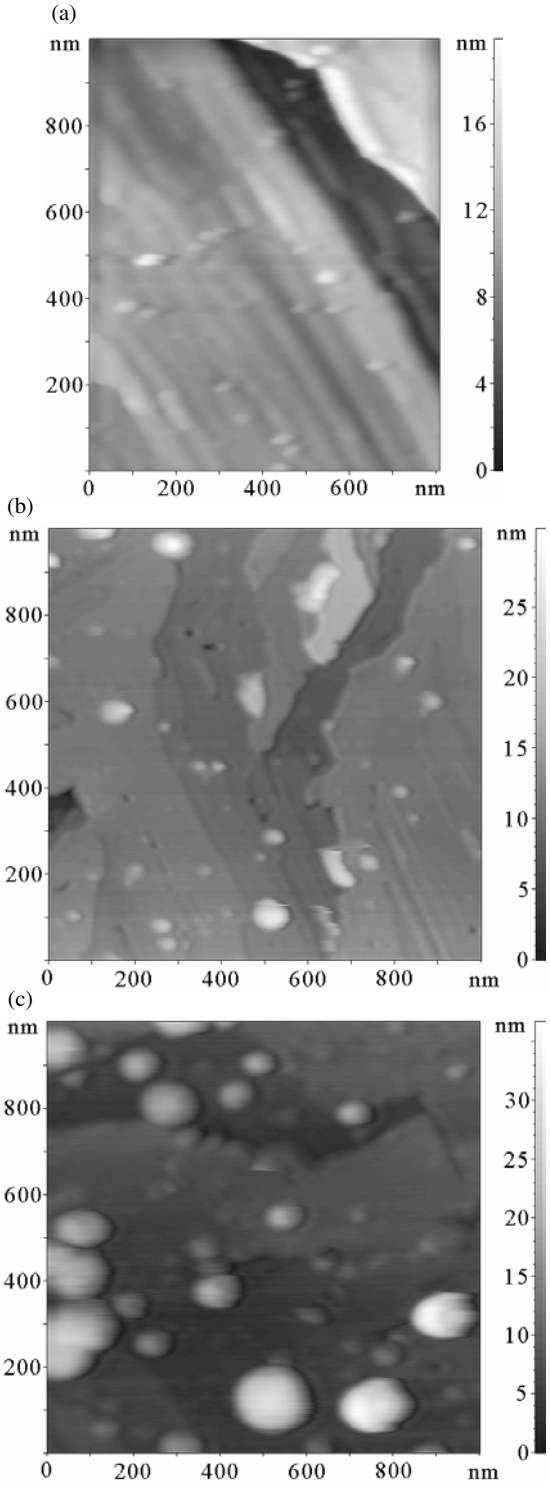

Figure 2. AFM images of samples irradiated up to different doses. (a) 50 MGy, $T_{irr} = 120\,^{\circ}C$, (b) 150 MGy, $T_{irr} = 100\,^{\circ}C$, (c) 200 MGy, $T_{irr} = 100\,^{\circ}C$.

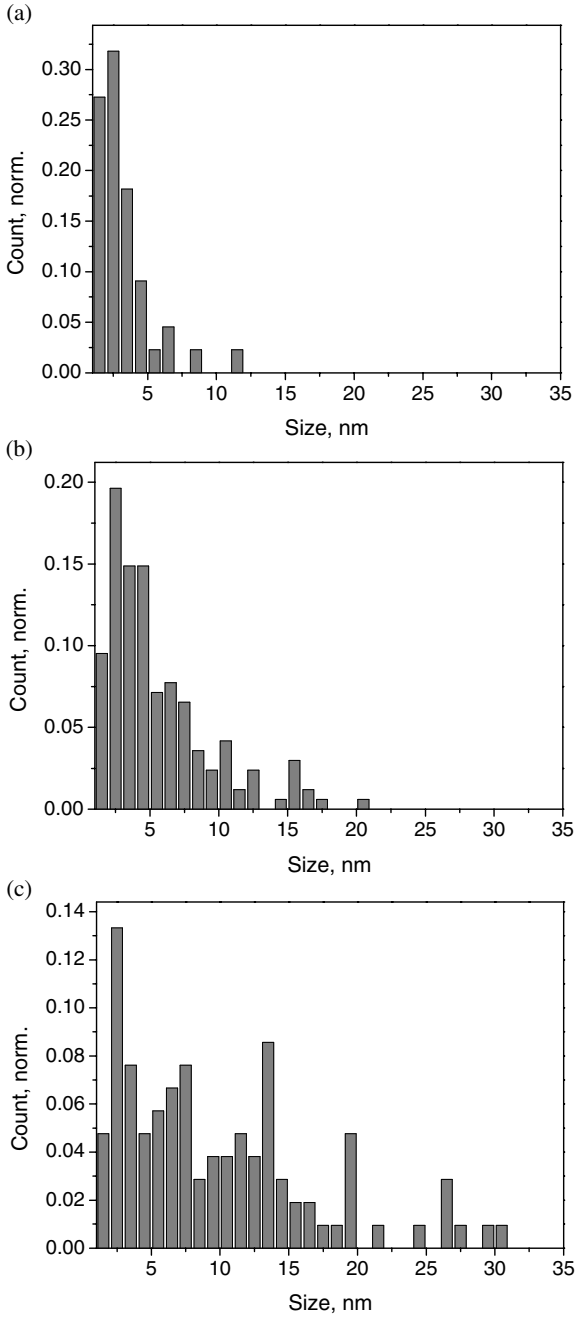

Figure 3. Distributions of protrusions in the z-direction (perpendicular to the scanned surface) for samples irradiated to different doses: (a) 50 MGy, (b) 150 MGy and (c) 200 MGy.

given by the function $F(R)$, which is normalized to the object number density

$$\int_0^\infty F(R)\,\mathrm{d}R = n_\mathrm{V} \tag{1}$$

where n_V is the volume concentration of the colloid particles.

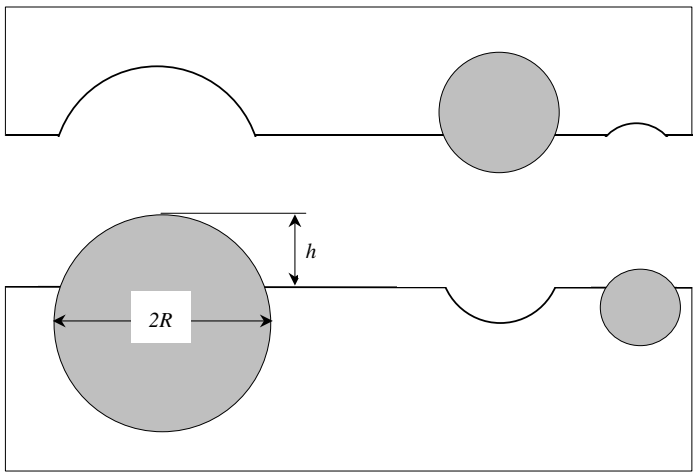

Figure 4. Schematic view of the AFM sample.

Similar to the experimental procedure the crystalline medium is cleaved along a plane such that the colloids are not cleaved. Because of the symmetry of the problem, it is assumed that a colloid with radius R can protrude above the surface to the maximum height $h_{\max} = R$. Otherwise the colloid remains in the upper part of the cleaved matrix (see figure 4).

During AFM scanning of the sample surface the data are collected, which are represented in the form of a distribution function of the protrusions $f(h)$ normalized to the surface number density of protrusions,

$$\int_0^\infty f(h)\,\mathrm{d}h = n_S \tag{2}$$

where n_S is the surface concentration of the colloid particles.

It can be shown that the 2D and 3D distribution functions are related by the expressions[5]

$$f(h) = \int_h^\infty F(R)\,\mathrm{d}R \qquad F(R) = -\frac{\mathrm{d}f(R)}{\mathrm{d}R}. \tag{3}$$

It follows from (3) that $f(h)$ decreases monotonously with increasing h since the distribution function $F(R)$ is positive by definition, i.e. the inequality $F(R) \geqslant 0$ must hold. This means that $f(h)$ has its maximum value at $h = 0$. Experimentally, the maximum is observed at about 2–3 nm because of the resolution limitations associated with the AFM experiment. Using (3) one can easily find the important relation between moments of the distributions functions

$$\langle h^n \rangle n_S = \frac{1}{n+1}\langle R^{n+1} \rangle n_V \tag{4}$$

where the angular brackets stand for the averaging with the appropriate distribution functions. Therefore the volume fraction of the colloids is written as

$$V_{\mathrm{col}} = \frac{4\pi}{3}\int_0^\infty R^3 F(R)\,\mathrm{d}R = 4\pi n_S \langle h^2 \rangle. \tag{5}$$

Together with the experimental data this formula can be used directly to estimate the volume fraction of the sodium colloids,

$$V_{\mathrm{col}}^{\mathrm{AFM}} = 4\pi \frac{N}{S}\frac{\sum_i h_i^2 n_i}{\sum_i n_i} \tag{6}$$

[5] The general mathematical aspects of the problem of relating the volume distributions of objects in a 3D medium to the surface distribution of cross-sections, obtained by a planar cutting of the medium, are considered in [6].

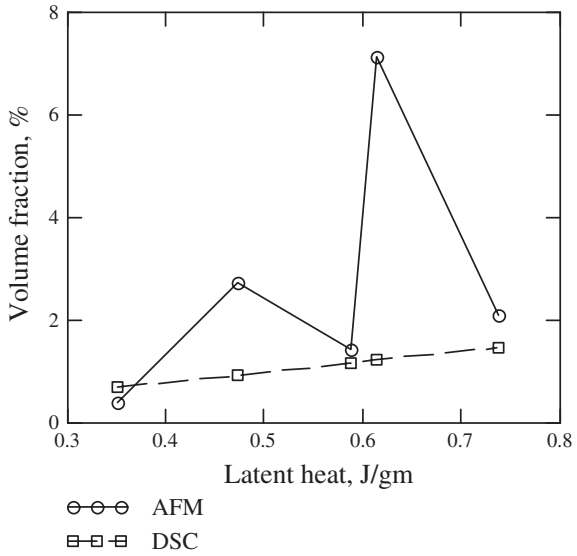

Figure 5. The dependence of the colloid volume fraction derived from (i) the AFM data (circles, equation (6)) and (ii) from the LHM of the Na colloids (squares, equation (7)).

where N is the total number of protrusions found by AFM, S is the scanned surface area and n_i is the number of protrusions of height h_i. The volume fraction of the metallic sodium in the sample can be also derived from the DSC data. This means that results obtained with two independent experimental methods can be cross-checked. The volume fraction of the metallic sodium is related to the total latent heat of melting (LHM) by

$$V_{\mathrm{col}}^{\mathrm{DSC}} = \frac{d_{\mathrm{NaCl}}}{d_{\mathrm{Na}}} \frac{Q}{H_{\mathrm{f}} m}, \tag{7}$$

where d_{NaCl} and d_{Na} are the densities of the matrix and metallic sodium, respectively; Q is the total measured LHM of metallic sodium, m is the sample weight and H_{f} is the specific heat of fusion. Here, it is assumed that the specific heat of fusion and the sodium density within the colloids does not depend on the colloid size.

Figure 5 shows the volume fraction of the colloids as a function of the corresponding LHM. It can be seen that the results obtained by two different methods correlate. However the scatter of data points is rather large, because of the poor statistics due to the limitations of the AFM method. Despite the lack of statistics we have tried to reconstruct the volume distribution functions for the samples irradiated up to doses of 50 and 150 MGy, which show good agreement between the DSC and the AFM measurements (the first and the third points in figure 5). The experimental histograms were fitted by the function

$$f(h) = \frac{2n_{\mathrm{S}}}{\alpha\sqrt{\pi}} \exp\left(-\frac{h^2}{\alpha^2}\right). \tag{8}$$

The corresponding 3D distribution function is given by

$$F(R) = \frac{4R}{\alpha^3\sqrt{\pi}} n_{\mathrm{S}} \exp\left(-\frac{R^2}{\alpha^2}\right). \tag{9}$$

The parameter α was adjusted to yield the same volume fractions of colloids as measured with AFM, i.e.

$$\frac{4\pi}{S}\sum_i h_i^2 n_i = \int_0^\infty \frac{4\pi}{3} R^3 F_V(R)\,\mathrm{d}R. \tag{10}$$

Figures 6(a) and (b) show the size distribution functions of the colloid protrusions above the cleaved matrix along with the fitting functions. Since $f(h)$ should reach its maximum value at $h = 0$, in order to obtain a good fit, the data measured by AFM were corrected, i.e. the maximum values in the experimental histograms were extrapolated along the x-axis to size zero (compare figures 3 and 6).

The fitting functions were used to evaluate the volume size distributions of the sodium colloids (figure 7). It is seen that the maximum of the distribution function shifts to larger sizes with increasing irradiation dose.

4. Discussion

The DSC scans of the irradiated samples which have been studied in this paper exhibit two melting peaks located at temperatures below the melting temperature of bulk sodium (figure 1). The relative magnitude of the heat flow associated with the peak located at higher temperature increases with the irradiation dose. There are three possibilities to explain this behaviour:

(1) It is known [7] that the melting temperature of a small metallic particle depends on particle radius. Therefore two melting peaks can be produced by an ensemble of particles with a bimodal distribution, i.e. with a well-defined double peaked distribution of particle sizes.
(2) The ensemble of colloids contains two populations of particle with two different structural states showing two different and well-defined melting temperatures.
(3) The colloids consist of two regions: (i) the inner part and (ii) the outer shell close to the NaCl–Na interface. For the reasons discussed below the area of the colloid close to the interface might be forced into the FCC structure, while the inner part has the BCC structure. This idea is supported by the results for Ni-nanoparticle-particles [8], which suggest that surface melting might occur.

According to our AFM results the size distribution function of Na colloids is unimodal for all samples investigated in this study (figure 7). Hence we can safely rule out the first possibility.

Our experimental observations strongly support either the second or the third possibility, i.e. the explanation for the appearance of the two different melting features in terms of the presence of two different structural states within the population of colloids. With the present information it is not possible to make a choice for either option 2 or 3. Because the situation of option 2 is the simpler one with only one adjustable parameter, we will focus our attention on option 2. Let us discuss the origin of these structural states. The crystal structure of bulk sodium at moderate temperatures is BCC (with a melting temperature of 97.87 °C). It is known for free sodium that in the case of small clusters sodium has a FCC lattice structure [1, 2]. This could also be the case for small sodium colloids in the NaCl host lattice. Under irradiation colloids are formed in NaCl by agglomeration of radiation-induced F centres [9], which topologically are the vacant sites in the Cl sublattice. Therefore, a small colloid represents a void in the Cl^- sublattice, or a Na cluster with a FCC lattice in real space. In other words small colloids inherit the FCC structure of the surrounding Na sublattice in the NaCl matrix. It is likely that up to a certain radius R_{trans}, the surrounding NaCl matrix forces an FCC Na colloid to keep its 'wrong' lattice structure. During irradiation this small colloid grows larger and its

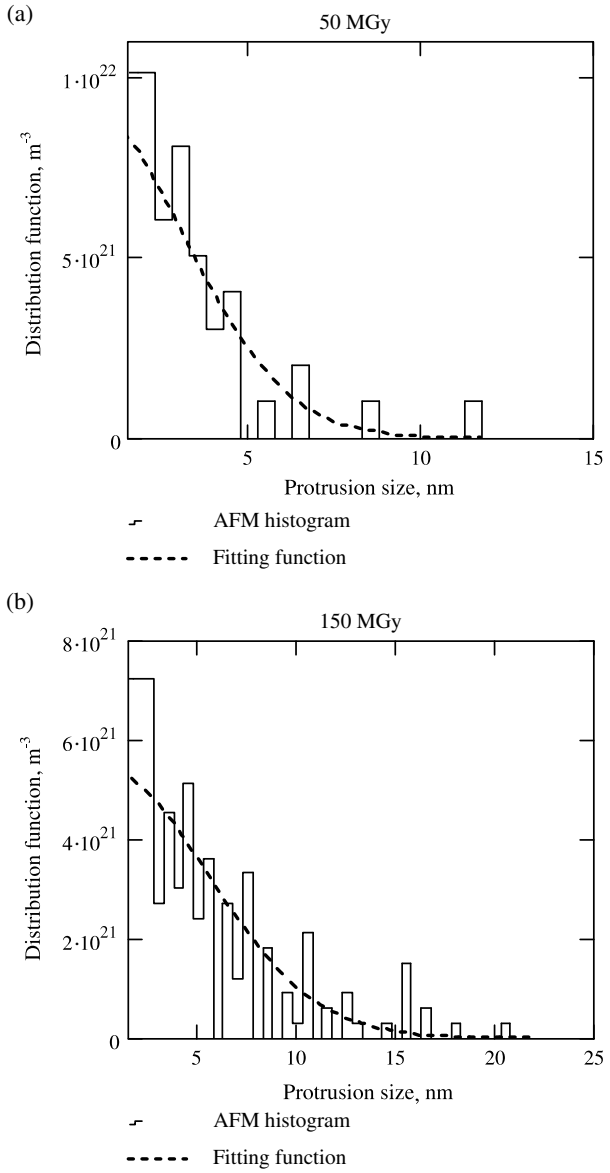

Figure 6. Size distribution functions of the colloid protrusions above the cleaved matrix measured by AFM after irradiation to 50 MGy (a) and 150 MGy (b). The dashed curves are the fitting functions given by (8) with $\alpha = 4.3$ nm (a) and $\alpha = 8$ nm (b). The distributions are normalized to the surface density (see (2)).

lattice eventually transforms into a BCC lattice[6] [10]. This means that the irradiated sample contains FCC colloids ($R \leqslant R_{\text{trans}}$) and BCC colloids ($R > R_{\text{trans}}$), the melting temperatures

[6] It should be mentioned that the lattice transformation of embedded particles was observed in metallic systems. For example, ion implantation of pure aluminium with thallium gives rise to the formation of nanoparticle-sized thallium inclusions [11]. Investigations have shown that these inclusions can have either a FCC or a BCC structure. Small inclusions (with diameters less than about 10 nm) are almost always FCC while larger inclusions (diameter larger than about 10 nm), are usually BCC [11].

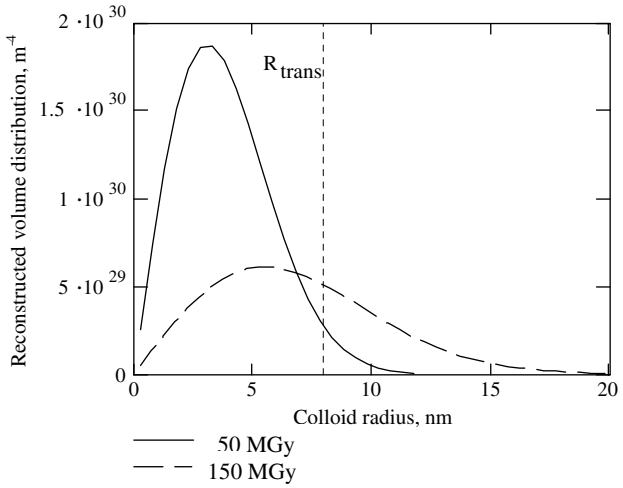

Figure 7. The volume distribution functions given by (9). The meaning of R_{trans} is explained in the text.

of which differ more than one could expect from the pure size effect. The melting temperature of large BCC colloids differs from the bulk melting temperature because of the size effect and the influence of the NaCl matrix.

Strictly speaking our reasoning is valid for NaCl samples which are subjected to irradiation at temperatures well below the temperature of the first melting peak, i.e. below 80 °C. The samples investigated in this paper were irradiated at temperatures higher than the melting temperature of bulk sodium. This means that during irradiation colloids were liquid. After irradiation the samples were cooled down to room temperature. The size-dependent crystal structures in colloids were formed during cooling. However, according to our previous results [9], the DSC scans of samples irradiated at low temperatures ($T < 80\,^{\circ}\text{C}$) and at high temperatures ($T \geqslant 100\,^{\circ}\text{C}$) are very similar. Moreover, the second DSC scan usually reproduces the same shape as the first one. These remarkable facts indicate that the structural states of colloids represent the equilibrium states. These states are determined by the properties of sodium clusters and the NaCl matrix.

The relative amount of heat required to melt colloids of the second type (BCC colloids) increases with increasing irradiation dose. This is explained naturally by the increase of volume fraction of BCC colloids due to their diffusion growth. The melting peaks are rather wide, probably because of the complicated size and shape dependence of the melting temperature of colloids.

The combination of AFM and DSC data allows us to estimate the transition radius R_{trans} between the two different structural states of the colloids. Let us assume that the melting temperatures of the colloids of the two types are distributed with density probability functions $\rho_{1,2}(T)$

$$\rho_{1,2}(T) = \frac{1}{\sigma_{1,2}\sqrt{2\pi}} \exp\left(-\frac{(T - T_{1,2})^2}{2\sigma_{1,2}^2}\right) \tag{11}$$

where T_1 and T_2 are the average melting temperatures which do not depend on the colloid radius; σ_1 and σ_2 are the standard deviations. The following numerical values are used below: $T_1 = 82\,^{\circ}\text{C}$, $T_2 = 92\,^{\circ}\text{C}$ and $\sigma_{1,2} = 2\,^{\circ}\text{C}$. We assume here that colloids with radii smaller than the transition radius R_{trans} produce the first melting peak at $T = T_1$, the other colloids

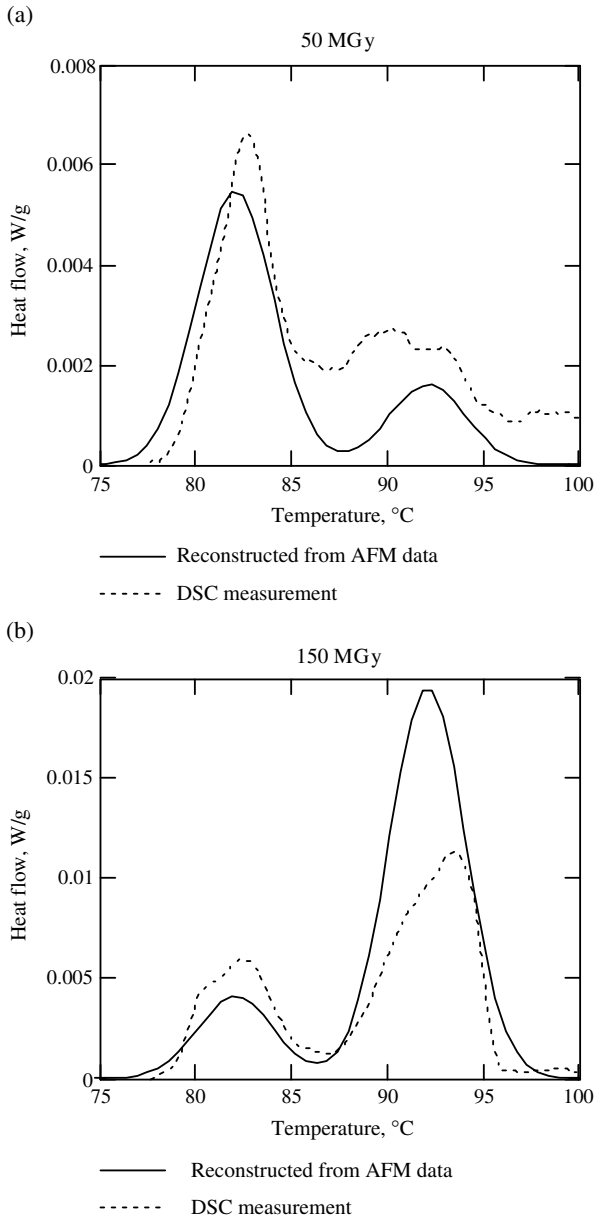

Figure 8. Comparison of experimental DSC curves with model DSC curves given by (12).

are responsible for the second melting peak at $T = T_2$. The heat flow as a function of the temperature is given by

$$q(T) = C\rho_1(T)\int_0^{R_{\text{trans}}} \frac{4\pi}{3} r^3 F(r)\,\mathrm{d}r + C\rho_2(T)\int_{R_{\text{trans}}}^{\infty} \frac{4\pi}{3} r^3 F(r)\,\mathrm{d}r \qquad (12)$$

where $C = \frac{\beta_{\text{DSC}} H_{\text{f}}}{d_{\text{NaCl}} v_{\text{Na}}}$, β_{DSC} is the heating rate during the DSC measurements and v_{Na} is the molar volume of Na. In equation (12) the first and the second terms represent the contributions to the heat flow associated with the colloids of the first and second types, respectively.

R_{trans} was adjusted to produce the temperature dependence of heat flow similar to what has been observed experimentally. In figure 8 we compare the experimental DSC curves with the reconstructed curves calculated with equation (12). According to our estimations, during colloid growth the transition to the BCC structural state occurs at $R_{\text{trans}} = 8$ nm. This estimation does not contradict the experimental melting results obtained for free sodium clusters [1, 2], where the transition radius has been evaluated to be about 3.5 or 4 nm, (cluster of about 10^4 atoms). We could expect a larger transition size for clusters embedded in a rigid NaCl matrix compared with free Na particles.

5. Conclusions

- The latent heat of melting has been measured for sodium clusters with sizes in the range between 0.5 and 30 nm, produced in NaCl crystals by means of electron irradiation up to a dose of 200 MGy. The DSC measurements of the irradiated samples have revealed two melting peaks located at temperatures below the melting temperature of bulk sodium.
- The sodium colloids have been visualized in AFM experiments and their size distributions have been evaluated for different samples as a function of the irradiation dose.
- To explain the melting behaviour of Na colloids the phenomenological model has been formulated which attributes each melting peak to the population of sodium colloids with a particular crystal structure. It is likely that the surrounding NaCl matrix forces the small sodium clusters to retain the FCC lattice of the Na sublattice. When a small colloid grows, its lattice eventually transforms into a BCC lattice of bulk Na.
- By comparison of the model results with the DSC measurements the transition radius between FCC and BCC structural states has been estimated to be 8 nm.
- The dose dependence of metallic sodium volume fraction measured with AFM shows a large scatter in comparison with the corresponding dependence obtained with DSC measurements (i.e. the DSC method is more precise). This increased scatter appears to be due to the poor statistics of the AFM method. Another reason might be that on the cleaved surface the shape and the arrangement of the sodium colloids differ from those in the bulk of the sample.

Acknowledgments

This work was supported by the Netherlands Organization for Scientific Research (NWO-Nederlandse Organisatie voor Wetenschappelijk Onderzoek) project number 047-008-021, the Russian Foundation for Basic Research project number NSh-1905-2003.2 and by the Science and Technology Center in Ukraine, STCU Project No 1761.

References

[1] Kusche R, Hippler Th, Schmidt M, von Issendor B and Haberland H 1999 Melting of free sodium clusters *Eur. Phys. J.* D **9** 1–4
[2] Martin T P, Naher U, Schaber H and Zimmermann U 1994 Evidence for a size-dependent melting of sodium clusters *J. Chem. Phys.* **100** 2322
[3] Reyes-Nava J A, Garzon I L, Beltran M R and Michaelian K 2002 Melting of sodium clusters *Rev. Mex. Fis.* **48** 450
[4] Johnston R L 1998 The development of metallic behaviour in clusters *Phil. Trans. R. Soc.* A **356** 211–30
[5] Seinen J 1994 *PhD Thesis* Rijksuniversiteit Groningen
[6] Kok L P 1990 *100 Problems of My Wife and Their Solution in Theoretical Stereology* (Leyden: Coulomb Press)
[7] Nagaev E L 1992 Equilibrium and quasiequilibrium properties of small particles *Phys. Rep.* **222** 199–307

[8] Qi Y, Cagin T, Johnson W L and Goddard W A III 2001 Melting and crystallization in Ni nanoclusters: the mesoscale regime *J. Chem. Phys.* **115** 385–94
[9] Dubinko V I, Turkin A A, Vainshtein D I and den Hartog H W 2002 Kinetics of nucleation and coarsening of colloids and voids in crystals under irradiation *J. Nucl. Mater.* **304** 117–28
[10] Sulyanov S N, Kheiker D M, Vainshtein D I and den Hartog H W 2003 Characterization of Na precipitates in electron irradiated NaCl crystals by wide angle x-ray scattering (WAXC) *Solid State Commun.* **128** 419–23
[11] Sorensen A H, Johnson E, Bourdelle K K, Johansen A, Andersen H H and Sarholt-Kristensen L 1997 Sizes, structures and phase transformations of nanosized thallium inclusions in aluminium *Phil. Mag.* A **75** 1533–52
[12] Groote J C, Weerkamp J R W and den Hartog H W 1991 An irradiation facility for radiation damage investigations *Meas. Sci. Technol.* **2** 1187–91
[13] Berger M J and Seltzer S M 1984 *ICRU* 37 (Washington, DC: ICRU)